Kara Sea freshwater dispersion and export in the late 1990s

I. H. Harms

Zentrum für Meeres- und Klimaforschung, Institut für Meereskunde, Universität Hamburg, Hamburg, Germany

M. J. Karcher[1]

Alfred-Wegener-Institut für Polar und Meeresforschung, Bremerhaven, Germany

[1]   A regional coupled ice-ocean model for the Kara Sea, forced with boundary conditions from a large-scale North Atlantic/Arctic Ocean Model, is used to study dispersion and export of freshwater from Ob and Yenisei rivers toward the Arctic Ocean and the Laptev Sea, for the period 1996–2001. The years 1998 and 1999 were characterized by a strong positive sea level pressure (SLP) anomaly in the Siberian part of the Arctic Ocean. Owing to prevailing northeasterly winds, the SLP anomaly caused a blocking situation, which suppressed the otherwise eastward freshwater export to the Arctic Ocean and Laptev Sea. This reversal of the prevailing circulation scheme led to a dramatic freshening of the Kara Sea through accumulation of low-saline river water in the central and western parts. Additionally, the Kara Strait inflow from the Barents Sea, which presents the main source for saline Atlantic derived water, was reduced and partly even reversed. The suppressed freshwater export during winter 1998/1999 recovered in the following winter 1999/2000 when a significant pulse of low-saline surface water left toward the Laptev Sea. The variability of the river discharge plays a minor role for the investigated period because the interannual variability of runoff rates is generally too low to explain the observed hydrographic changes. The results underline the importance of local shelf sea processes for the variability of the freshwater export from the Arctic Shelves to the central Arctic Ocean.

Citation: Harms, I. H., and M. J. Karcher (2005), Kara Sea freshwater dispersion and export in the late 1990s, *J. Geophys. Res.*, *110*, C08007, doi:10.1029/2004JC002744.

1. Introduction

[2]   The present study investigates the freshwater export from the Kara Sea during the years 1996–2001, using two hydrodynamic coupled ice-ocean models with different domains and resolutions. The main focus of the study is on an unusual sea level pressure (SLP) pattern in the years 1998/1999, which consisted of a high-pressure anomaly over the northern Kara and eastern Barents seas. This anomaly had great influence on the Kara Sea flow fields and the exchange with the adjacent areas.

[3]   The export of freshwater from shelf areas, in liquid form or as sea ice, is a key process that determines the amount of freshwater stored above the Arctic Ocean's halocline and in the ice shield. The magnitude and the variability of this freshwater pool has been studied intensively during the last years because the release of freshwater from the Arctic Ocean to the Nordic Seas and the Labrador Sea is supposed to affect the global ocean's thermohaline circulation [e.g., *Häkkinen*, 1999; *Haak et al.*, 2003]. Recent speculations on increasing river discharge [*Peterson et al.*,

2002] in connection with atmospheric warming underline the urgent need to investigate in more detail the freshwater balance of Arctic Shelf Seas.

[4]   Understanding the freshwater dynamics of the Arctic Ocean requires a closer look at the shallow Eurasian shelf regions because here most of the river water enters and large amounts of ice are formed or melted. The shelf regions are exposed to seasonal and interannual atmospheric variability which affects circulation, hydrography, ice formation, and water mass transformation [e.g., *Schauer et al.*, 2002; *Harms et al.*, 2005]. Through these processes, atmospheric anomalies influence the characteristics and the intensity of the outflowing water masses from the shelves [*Karcher at al.*, 2003a, 2003b]. The Arctic Shelf Seas thus have a strong potential for modifying the freshwater signal that finally enters the Arctic Ocean.

[5]   The Kara Sea, together with the Laptev Sea, the East Siberian Sea and the Chukchi Sea, belongs to the Eurasian Arctic Shelf margin (Figure 1a). The Kara Sea receives roughly one third of the yearly total Arctic river water ($\sim$1200 km^3), mainly through the Ob and Yenisei rivers that drain a catchment area in Siberia and Russia of more than 5 million km^2. Approximately 80% of the river water is discharged in spring (May–June) [*Pavlov and Pfirman*, 1995] which leads to peak runoff rates of more than 10^5 m^3/s (e.g.,Yenisei).

---

[1]Also at Ocean-Atmosphere-Systems (O.A.Sys), Hamburg, Germany.
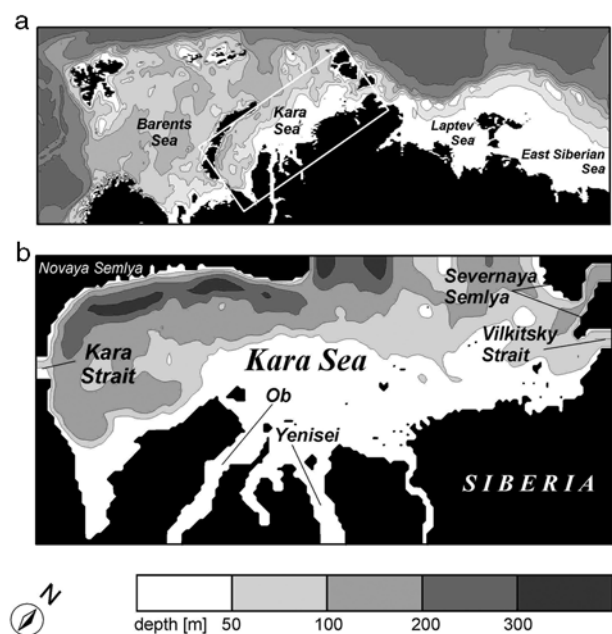
Figure 1. (a) Location of the Kara Sea Model domain on the Arctic Shelf and (b) topography of the regional Kara Sea Model.

[6] The Kara Sea is known for its large ice production, mainly along the shallow Taymyr coast. Freezing rates are much higher than corresponding melting rates, which implies that large amounts of freshwater leave the area in form of sea ice. *Pavlov et al.* [1993] estimated the sea ice export toward the central Arctic Ocean to be around 150 km^3/yr.

[7] Being close to the Barents Sea, the Kara Sea is also influenced by an inflow of relatively warm and saline water masses of North Atlantic origin that enter through the Kara Strait. The simulated annual average inflow is in a range of 0.2–0.3 Sv. However, owing to the seasonal variability of the wind field, the Atlantic inflow is strong only in winter whereas it is much weaker or even blocked in summer [*Harms and Karcher*, 1999].

[8] In section 2 we describe the two numerical models used in the present study. Following an analysis of the large-scale circulation patterns on the Eurasian Shelf in relation to SLP patterns from 1948–2002 (section 3.1), we present the circulation of the Kara Sea in the late 1990s in more detail (section 3.2) and discuss the consequences for freshwater dispersion and export (section 3.3).

2. Model Configurations

2.1. Regional Kara Sea Model

[9] A hydrodynamic, 3-D, coupled ice-ocean model is applied to the Kara Sea (Figure 1b) with a horizontal grid resolution of 9.4 km. The model is based on the coding of the Hamburg Shelf Ocean Model HAMSOM, introduced by *Backhaus* [1985], and previously applied to the Kara Sea by *Harms and Karcher* [1999] and *Harms et al.* [2000, 2003]. In these previous applications, the model was intensively validated.

[10] The HAMSOM code is based on nonlinear primitive equations of motion, invoking the hydrostatic approximation and the equation of continuity, which predicts the elevation of the free surface from the divergence of the depth-mean transport. The numerical scheme is semi-implicit and the equations are discretized as finite differences on an Arakawa C-grid [*Stronach et al.*, 1993]. The circulation model is coupled to a thermodynamic and dynamic sea ice model, which calculates space- and time-dependent variations of ice thickness and ice concentration [*Hibler*, 1979]. Sea surface heat fluxes, calculated with bulk formulae [*Maykut*, 1986], are used to determine prognostically the ocean temperature and thermodynamic ice formation [*Parkinson and Washington*, 1979]. Salt fluxes due to brine and freshwater release are proportional to thermodynamic ice growth [*Lemke et al.*, 1990].

[11] The Kara Sea model is forced with realistic atmospheric winds, heat fluxes, river runoff and tides.

[12] 1. Atmospheric data such as surface wind stress, air temperature, humidity, and cloud cover is taken from the NCEP database for the years 1996–2001 [*Kalnay et al.*, 1996].

[13] 2. The river runoff data for the Ob (including the tributaries Taz and Pur), Yenisei, and Pyasina is given as daily mean volume fluxes in m^3/s. A large part of this data was taken from the R_ArcticNET-database (A Regional, Hydrometeorological Data Network for the pan-Arctic Region, http://www.r-arcticnet.sr.unh.edu/abstract.html). Several time gaps had to be filled in order to get a continuous time series. This was done partly by fitting climatological data into the gaps.

[14] 3. The Kara Sea Model accounts for the dominant M$_2$-tidal constituent. Amplitudes and phases were taken from tidal models of the Arctic Ocean [*Gjevik and Straume*, 1989; *Kowalik and Proshutinsky*, 1993, 1994] and applied to the open boundaries. A detailed description of the tidal solution is given by *Harms and Karcher* [1999].

[15] 4. The open boundaries in the Kara Sea model are composed of (1) the Kara Strait, (2) the northern opening between Novaya Semlya and Severnaya Semlya, and (3) the Vilkitzky Strait in the east (Figure 1b). At all open boundaries, the sea surface elevations are prescribed. They consist of tidal elevations, the long-term far field sea surface variability (from NAOSIM, see below), and a baroclinic adjustment that accounts for horizontal density gradients along the boundary.

[16] A well-known problem with NCEP data is the too low cloud coverage which caused a significant underestimation of the summer ice extent in the model. The original NCEP cloud cover data were therefore increased throughout the model domain by 25%, and the model results were compared to SSMI satellite data observations [*Kern and Harms*, 2004]. The comparison reveals a much better agreement between model results and observations than without correction, in particular during freezing in autumn. Also, the opening and closing of polynyas is well reproduced with that simple correction. However, smaller discrepancies can still be found in spring when short- and long-wave radiation, which strongly depend on the cloud cover, play a dominant role in melting the ice.

[17] The river inflow is prescribed actively as a volume flux in m^3/s at the grid point where the river enters the sea.

The salinity at these points is kept to zero. Apart from the impact on salinity and density, the river water thus has an additional dynamic effect through the surplus of mass added to the model. Precipitation and evaporation were neglected because both parameters are small and mostly balanced throughout the model domain.

[18] The Barents Sea inflow through the Kara Strait is of major importance because it brings heat and salt into the Kara Sea. To account for these effects, monthly mean net inflows or outflows through the Kara Strait were prescribed from the larger-scale AWI/NAOSIM coupled ice-ocean general circulation model for the Arctic and sub-Arctic domain [Karcher et al., 2003a]. These volume fluxes were transformed into daily mean sea surface elevations and prescribed at the open boundary in the Kara Strait.

[19] Inflow or outflow is thus prescribed explicitly only for the Kara Strait and the rivers. At the two other open boundaries, no explicit sea surface elevations are prescribed, except tides and the adjustment due to horizontal density gradients. These boundaries are "free" in terms of volume flux and allow for a compensation of the two flux constraints and dynamic effects described above. Temperature and salinity at open boundaries follow a zero gradient condition while there is outflow (dT/dn = 0), whereas during inflow the values are reset to initial boundary values.

[20] The simulation of the 1996–2001 period was started at 1 September 1995 using the initial conditions from previous climatological simulations [Harms et al., 2003]. The climatological spin-up was run for 3 years in a fully prognostic mode in order to achieve a cyclic stationary state. For the climatological spin-up, a relaxation of salinity to the initial data was applied in order to avoid a drift toward higher salinities that was observed without relaxation. We attribute this effect to an underestimated climatological runoff compared to the intense salt release from ice formation. The interannual runs (1996–2001) are completely free of any relaxation. More details on the climatologically forced results are given by Harms and Karcher [1999].

2.2. NAOSIM

[21] The NAOSIM (North Atlantic/Arctic Ocean-Sea Ice Model) has been developed at the Alfred-Wegener-Institute for Polar and Marine Research, Germany, for the purpose of high-latitude studies of ocean climate [Gerdes et al., 2005; Karcher et al., 2003a, 2003b; Kauker et al., 2003]. The ocean circulation model is derived from the GFDL modular ocean model MOM-2 [Pacanowski, 1995]. The model domain includes the Atlantic Ocean north of approximately 50°N, the Nordic Seas, and the Arctic Ocean.

[22] The model is formulated on a rotated spherical grid with a horizontal resolution of 0.25° and 30 unevenly spaced levels in the vertical. The bottom topography is based on the Etopo5 data set of the National Geophysical Data Center. Modifications were made to two open channels in the Canadian Archipelago connecting the Arctic Ocean with Baffin Bay.

[23] For the advection of potential temperature, salinity, and other tracers, an FCT-scheme [Gerdes et al., 1991] is employed, which is characterized by a low implicit diffusion while avoiding false extrema ("overshooting") in advected quantities. There is no explicit diffusion acting on the tracers. A dynamic-thermodynamic sea ice model

with viscous-plastic rheology [Hibler, 1979] is coupled to the ocean model. The surface heat flux is calculated from standard bulk formulae using prescribed atmospheric data and sea surface temperature predicted by the ocean model. At the surface, a restoring flux based on an adjustment timescale of 180 days is applied.

[24] The initial conditions for potential temperature and salinity were taken from the Arctic Ocean EWG-climatology for winter [NSIDA Environmental Working Group, 1997]. Outside of the EWG-climatology domain, the climatology of Levitus and Boyer [1994] and Levitus et al. [1994] have been used. After a 50-year spin-up forced with climatology, the forcing consists of daily mean atmospheric data from the NCEP reanalysis for the period 1948–2001 [Kalnay et al., 1996]. Further details on the present implementation of the model are given by Kauker et al. [2003] and Gerdes et al. [2005].

3. Model Results

3.1. Eurasian Shelf: Long-Term SLP and Circulation Patterns

[25] Analysis of the SLP in the vicinity of the Kara Sea over the period 1948–2002 reveals a strong positive anomaly over the northeastern Barents Sea and the Kara Sea in the years 1998 and 1999. The effects of this anomaly, however, were not restricted to the Kara Sea alone. Empirical orthogonal function (EOF) analysis of the simulated oceanic flow fields of the entire Barents and Kara Sea shelf over the period 1948–2002 reveals two dominant modes that explain 43% and 25% of the variability, respectively. This result is very similar to an analysis carried out for the period 1979 to 2002 based on an ECMWF-forced run of the same large-scale model [Karcher et al., 2003b]. The first mode (not shown here) describes a general increase of the through-flow from the Barents Sea Opening eastward, including the Kara Sea. The second mode describes a northward shift of the through-flow through the Barents Sea, and reduction of eastward flow through the Kara Strait and the Kara Sea (Figures 2a and 2b). This mode was strongest in the years 1998/1999, when circulation and transport rates in the Kara Sea were completely reversed. The mode is also persistently positive, though somewhat weaker, during the late 1950s and early 1960s.

[26] Yearly mean SLP data have been regressed on the second-mode principal component of the oceanic velocities shown above. The resulting SLP pattern exhibits a tripole with a high-pressure anomaly over the eastern Barents Sea and the Kara Sea and low pressure over Iceland and the Bering Sea (Figure 2c). The large-scale character of this anomalous SLP pattern in the late 1990s is also highlighted by the results of a combined analysis of the 1979–2001 sea-ice concentrations from SSMI satellite data and the NAOSIM simulation also used in the present study [Kauker et al., 2003]. The second mode for the winter season found by Kauker et al. [2003] by using a maximum covariance analysis (MCA) revealed the existence of a sea-ice concentration dipole with a maximum in the southeastern and a minimum in the northeastern Barents Sea. The associated sea-ice drift anomaly is directed from the Kara Sea via Kara Strait into the Barents Sea and consists of an Arctic basin wide intensification of anticyclonic ice motion. This mode
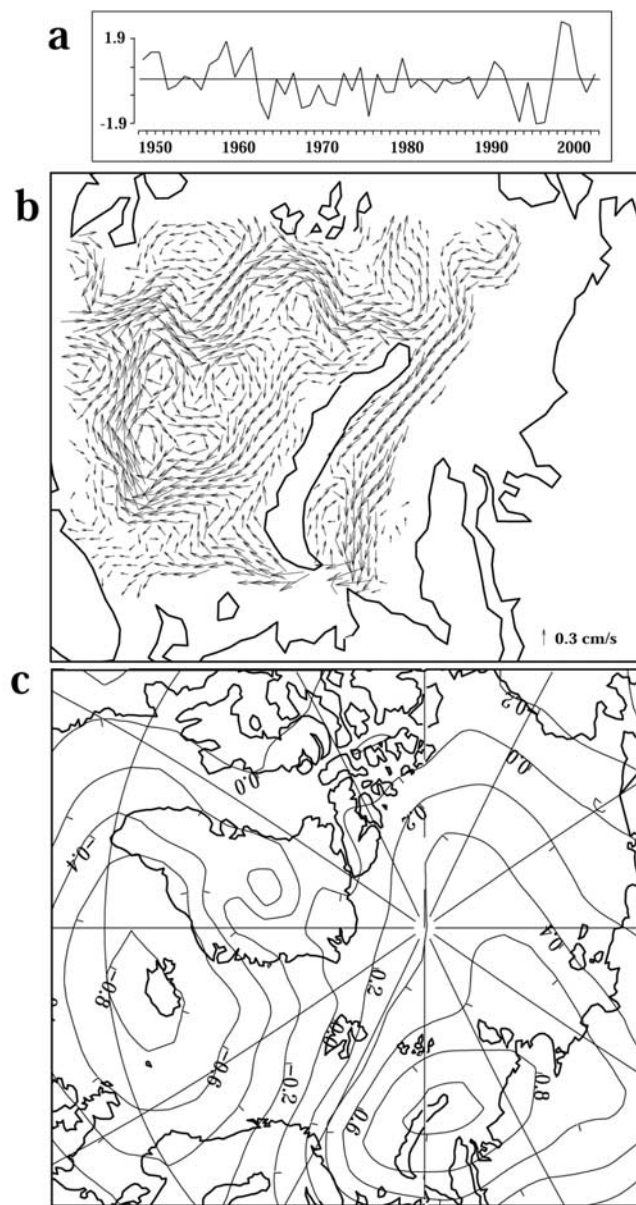
Figure 2. Second EOF mode of yearly mean velocities in 80 m depth on the Barents and Kara shelf for the period 1948–2002: (a) principal component and (b) circulation pattern. (c) SLP pattern associated with the second mode (based on yearly mean SLP data from the NCEP reanalysis).

has its strongest positive state in the winter 1998/1999. It is associated with a SLP anomaly pattern with a maximum over the Kara Sea and minima over the Bering Sea and the North Sea, very similar to the second mode of the oceanic flow fields on the shelf found in the present study.

## 3.2. Kara Sea: Circulation and Volume Fluxes 1995–2001

[27] The air pressure distribution and hence the wind system over the Kara Sea is characterized by large seasonal variability, similar to a monsoon regime. The summer is dominated by easterly winds due to high pressure over the central Arctic and low-pressure cells over the Siberian

mainland. In winter, the situation is almost reversed. High pressure develops over the continental landmasses of Siberia whereas low-pressure systems move frequently from the Barents Sea region into the Kara Sea. This results in stronger west to southwest winds during winter [*Harms and Karcher*, 1999].

[28] The positive SLP anomaly in winter 1998/1999, however, blocked the penetration of low-pressure systems toward the Kara Sea whereby the westerly winds were suppressed and unusual easterly winds developed during that time. The consequences of this anomalous atmospheric circulation are in particular detectable in reversed volume fluxes through the important inflow and outflow regions such as the Kara Strait or the Vilkitzky Strait.

[29] The Kara Strait through-flow (Figure 3a) presents an important source for Atlantic water masses entering the Kara Sea. Yearly mean transport rates are predominantly positive from the Barents Sea toward the Kara Sea, however, with a distinct seasonal modulation. Monthly mean values (Figure 3b) reveal that the inflow is usually strong during winter and weaker or even negative during summer which is basically an effect of the seasonally varying wind field [*Harms and Karcher*, 1999]. A significant deviation from this prevailing seasonal modulation is visible in 1998/1999 when owing to the SLP anomaly, the flow from the Barents to the Kara Sea through the Kara Strait is reversed over a period of 17 months.

[30] The monthly mean NAOSIM transport rates from Figure 3b are used, together with other forcing data sets (local atmospheric data, runoff, and tides) to run the regional scale Kara Sea model over the period 1995 to 2001. The time series of simulated transport rates through the Kara Strait, the Vilkitzky Strait and the open northern boundary toward the Arctic Ocean (Figure 4) indicate that
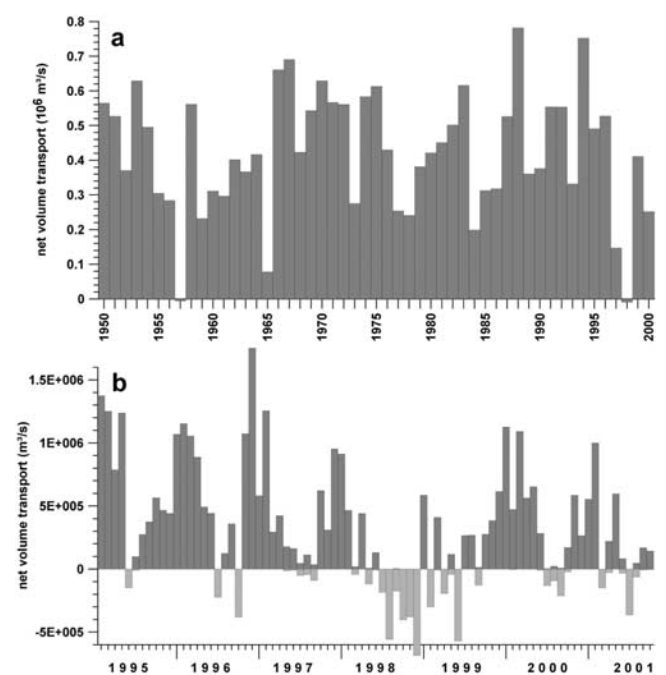
Figure 3. (a) Yearly mean Kara Strait throughflow from 1948–2001 and (b) monthly mean Kara Strait throughflow from 1995–2001, deduced from NAOSIM.
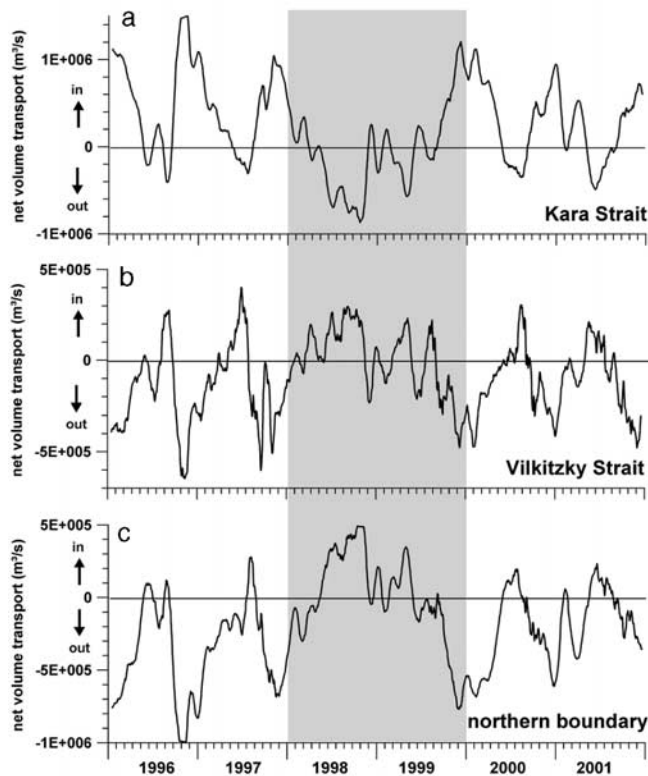
Figure 4. Simulated net volume transport through (a) Kara Strait, (b) Vilkitzky Strait, and (c) the northern model boundary, between Novaya Semlya and Severnaya Semlya.

anomalous fluxes in 1998/1999 can be observed for all three open boundaries.

[31] The volume flux through the Kara Strait (Figure 4a) is dominated by strong seasonal variability. Usually, enhanced inflow from the Barents Sea during winter due to prevailing southwesterly winds alternates with an occasional outflow due to dominating easterly winds in summer. However, an exceptional strong outflow occurs during summer and autumn 1998 which is followed by exceptional weak inflow during the winter 1998/1999.

[32] The main outflow to the east is through Vilkitzky Strait (Figure 4b) between Severnaya Semlya and Cape Tscheljushkin, the link between Kara and Laptev Sea. Here, usually, the outflow dominates in autumn and winter and only a small inflow occurs during summer. The open northern boundary (Figure 4c) between Novaya Semlya and Severnaya Semlya has a similar behavior, strong outflow in autumn and winter and small inflow in summer. The shaded area in Figure 4 highlights that both openings, to the north and to the east, are significantly affected by the atmospheric anomaly in winter 1998/1999 in a way that the usual outflow is blocked or even reversed.

## 3.3. Kara Sea: Freshwater Dispersion and Export 1995–2001

[33] The anomalous volume fluxes through the main openings suggest a largely reversed circulation regime which was present in the Kara Sea in winter 1998/1999. These changes had consequences for the coastal freshwater

dispersion and finally also for the freshwater outflow to the Arctic Ocean and the Laptev Sea.

[34] Under normal conditions, freshwater from the river runoff peak in spring accumulates at the surface of the central Kara Sea, mostly as a large plume in front of the estuaries. The plume area varies, but the largest extent is typically reached in midsummer. In late summer/autumn, the river plume starts to move eastward along the Siberian coast (Figure 5). The strongest outflow of freshwater from the Kara Sea occurs in autumn and winter, through Vilkitzky Strait. The western parts of the Kara Sea are typically less affected by freshwater [*Harms and Karcher*, 1999; *Harms et al.*, 2000].

[35] The anomalous circulation and volume flux during the years 1998/1999 changed this hydrographic situation in the Kara Sea dramatically. In particular, the dispersion of river water from the Ob and the Yenisei was significantly affected. In order to visualize the change in the freshwater distribution in time, Figure 6 shows the extent of the low-saline surface water plume with salinities less than 30 kg/m^3 in three compartments, the western, the central, and the eastern Kara Sea.

[36] The central Kara Sea (Figure 6a) shows during the highlighted period of interest basically a negative trend. A large, long-lasting plume extent in summer 1998 is followed by a lower extent in summer 1999 and an extreme low value in winter 1999/2000. The opposite trend is visible for the western Kara Sea (Figure 6b), where the maximum plume extension in autumn increases steadily from 1996 on. The winter minimum extension is almost absent in 1998/1999, and the extreme high value in autumn 1999 drops dramatically toward the following winter 1999/2000. In the eastern Kara Sea (Figure 6c), however, the winter 1998/1999 is characterized by an extremely small plume extent.
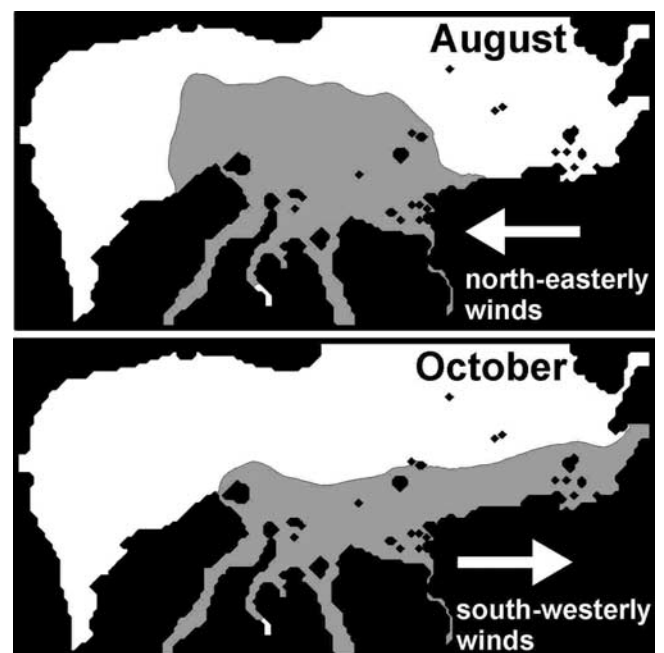
Figure 5. Surface plume extent (salinity < 30 psu) in the Kara Sea during midsummer (August) and in autumn (October), deduced from climatological simulations.
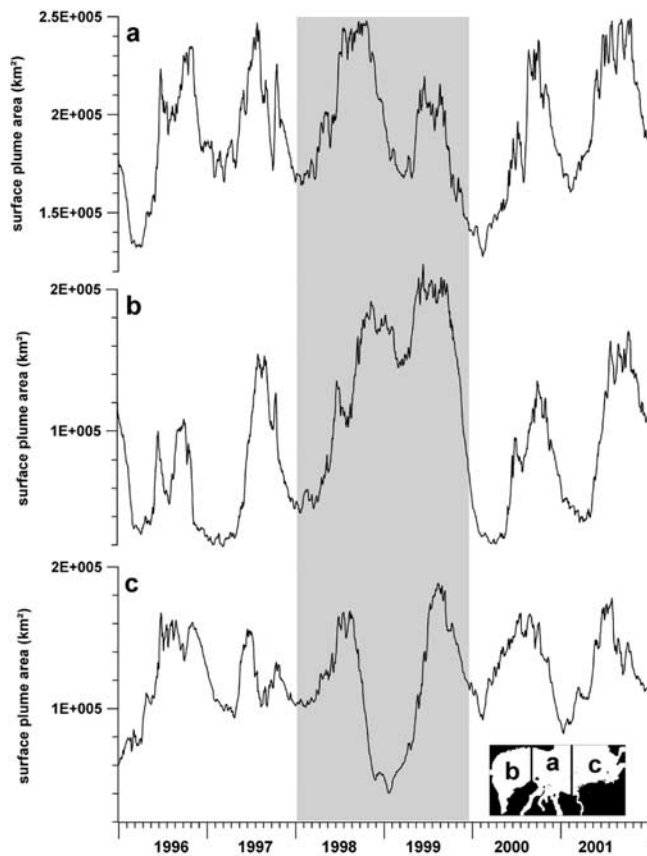
Figure 6. Simulated surface plume extent (salinity < 30 psu) (a) in the central Kara Sea, (b) in the western part, and (c) in the eastern part.

[37] The reason for the unusual seasonal cycle in the river water distribution in the Kara Sea is the anomalous winter SLP pattern in 1998/1999. Owing to prevailing northeasterly winds, the usual flushing of freshwater toward the east fails completely for autumn 1998 and winter 98/99. The freshwater in the eastern part is thus depleted whereas the western parts show an increase of riverine freshwater. The spring runoff in 1999 delivers even more river water to the western parts, leading to a distinct maximum extent in the west, in summer 1999.

[38] This situation lasts until autumn 1999, when the winds returned to normal winter conditions with prevailing westerly directions. This change in atmospheric conditions induces a strong flushing of the western and central parts of the Kara Sea, whereby the plume extent in the west drops dramatically. Large amounts of low-salinity surface waters are pushed along the Siberian coast toward the east. In the course of this flushing, an unusually large pulse of low-salinity water leaves the Kara Sea toward the Arctic Ocean and the Laptev Sea in autumn 1999 and winter 1999/2000. The anomalous low salinity is visible in Hovmoeller diagrams of salinity profiles in the main freshwater exits near Severnaya Semlya and in the Vilkitzky Strait (Figures 7a and 7b). In particular, in the Vilkitzky Strait (Figure 7b), a pulse of very low salinity water extending down to about 20 m depth occurs in 1999/2000 whereas the previous winter 1998/1999 is characterized by anomalously high salinities.

[39] Time series of the freshwater export through the northern opening and Vilkitzky Strait (Figure 8) demonstrate the evolution of the blocking and flushing events between 1998 and 2000. Daily mean values as well as yearly values of the freshwater export, relative to 34.8 kg/m^3 salinity, show that in both openings the export of freshwater is almost absent in winter 1998/1999. Values are either close to zero or partly even negative (not shown), which denotes either a negative net volume transport into the Kara Sea or a mean salinity at the boundary higher than the reference value of 34.8. The extreme low export is followed by a distinct flushing event in 1999/2000 which is very pronounced in the Vilkitzky Strait. Here the accumulated yearly export is twice as high as in 1996/1997 and 1997/1998.

4. Discussion

[40] Our model results show that circulation and hydrography in the Kara Sea are strongly affected by an atmospheric pressure anomaly over the northern Barents and Kara Seas in winter 1998/1999. The local positive SLP anomaly is part of a large-scale SLP pattern which is evident in the analysis of ocean velocities on the Siberian shelves and in ice cover data by *Kauker et al.* [2003]. The main local effect of this pressure anomaly is a weakening of the northeastward transport of river water through the Kara Sea due to a change in the dominant wind directions. As a result, the freshwater export to the north and east is almost blocked from mid-1998 to mid-1999, and the river water starts to accumulate in central and southwestern parts of the Kara Sea. The blocking situation ceases in late 1999 when the winds return to normal winter conditions and the Kara Sea is flushed. A large pulse of low-salinity water carrying the excess freshwater which had been previously blocked
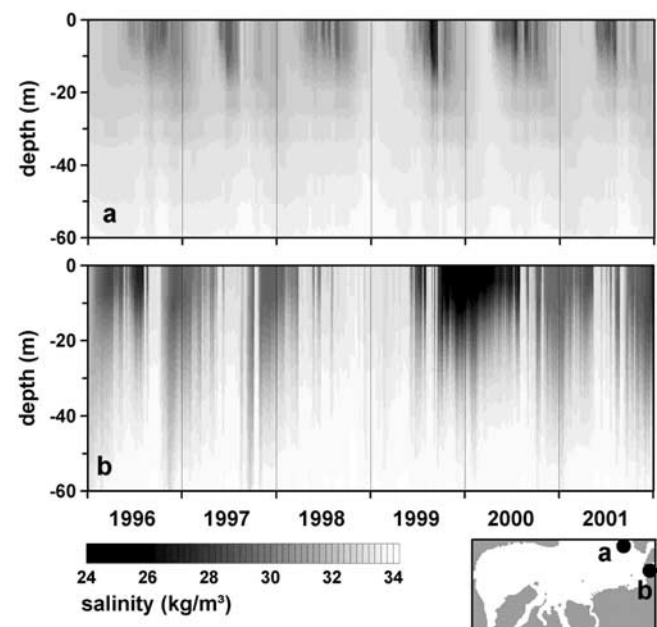
Figure 7. Hovmüller diagram of simulated salinity profiles from 1996–2001, (a) near Severnaya Semlya and (b) in the Vilkitzky Strait.
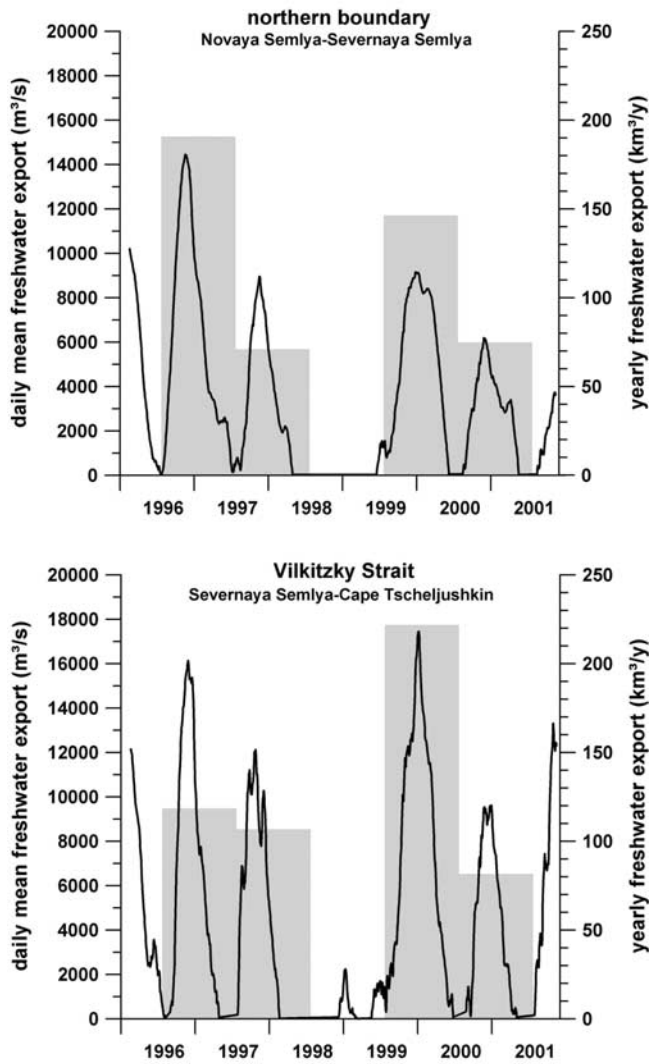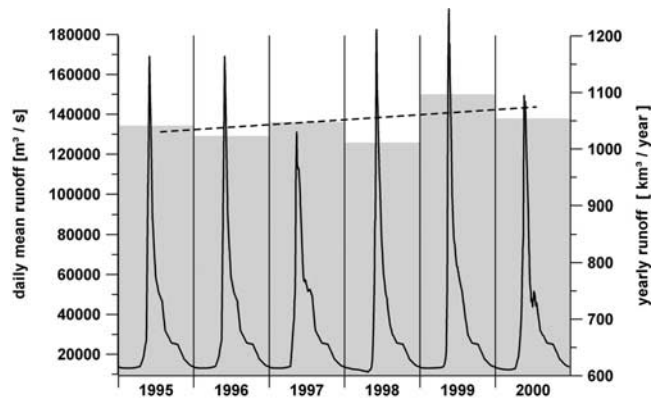
Figure 8. Simulated daily mean freshwater export (solid line/left axis) and winter centered accumulated yearly freshwater export (bars/right axis) through the (top) northern boundary and (bottom) Vilkitzky Strait, relative to 34.8 kg/m³.

Figure 9. Ob and Yenisei daily mean runoff (solid line/left axis) and accumulated yearly runoff (bars/right axis). Dashed line shows the linear trend from 1995–2000.

eastern boundaries. The total freshwater content in the Kara Sea increased in 1999 by roughly 350 km³ relative to the mean of 1995–2001 (Figure 10). The rivers' contribution to this increase is not more than 100 km³ (see Figure 9), which is less than one third. The remaining surplus of 250 km³ additional freshwater in 1999 can be explained by the dramatic drop in freshwater export during the winter 1998/1999 which is in the range of 200–300 km³ for both open boundaries (see Figure 8).

[43] The simulated freshening of the Kara Sea is also supported by observations. *Simstich et al.* [2005] use proxy data from Arctic bivalve shells to determine interannual trends in the coastal waters of the Kara Sea. These proxy data are able to integrate changes in water mass characteristics over longer periods, i.e., years. Although the shells are attached to the bottom and hence only reflect changes in the bottom water mass characteristics, the proxy data reveal the same trend in freshening for the late 1990s as the model does, even if the absolute values for salinity at certain locations may differ. The fact that not only the surface waters became fresher in the late 1990s but also the bottom water masses leads to a drop of the average simulated

from outflow now leaves toward the Arctic Ocean and the Laptev Sea.

[41] The main reason for the large variability in the freshwater export can be found in the dynamic response of the Kara Sea to anomalous atmospheric conditions. The river runoff itself seems to play a minor role for the described changes because the interannual variability of the accumulated annual runoff is only less than 10% of its mean (Figure 9). During 1995–2000, the year 1998 shows the lowest annual discharge whereas the following summer 1999 has the highest amount of discharged river water from the Ob and Yenisei. In fact, the small positive trend of about 3% of the mean is caused mainly by the high discharge in 1999.
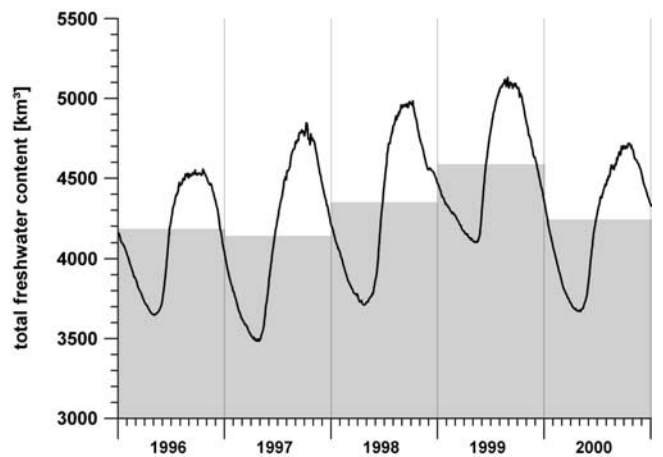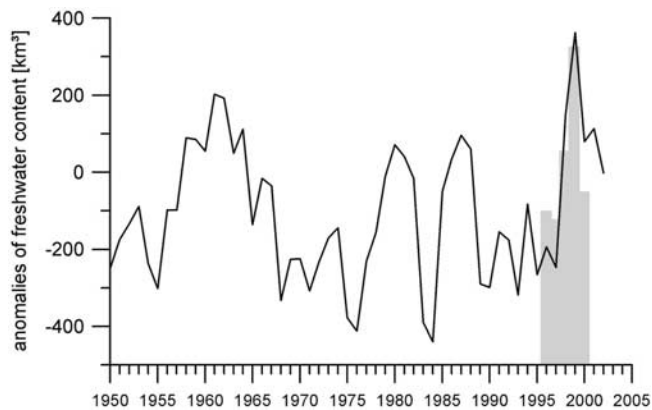
[42] The high runoff in 1999 probably supported the simulated freshening, but it clearly fails to explain the huge variability in the freshwater export over the northern and

Figure 10. Total freshwater content in the Kara Sea Model relative to 34.8. The curve presents daily mean values, and the bars are yearly means.

Figure 11. Anomalies of the freshwater content in the Kara Sea relative to the mean of 1995–2001 and a reference of 34.8. The curve presents yearly mean values from the NAOSIM, and the bars are yearly means from the regional Kara Sea model.

salinity in the Kara Sea by roughly 0.5 [c.f. *Simstich et al.*, 2005, Figure 10].

[44] The present model results show that the variability of atmospheric conditions can be more important for hydrographic changes in the Kara Sea than the frequently discussed change in the river discharge itself. Long-term analysis reveals that the SLP anomaly in winter 1998/1999 was not a unique event. In fact, the anomalies of the freshwater content in the Kara Sea from the NAOSIM had a peak also during the late 1950s and early 1960s, as Figure 11 demonstrates. This peak clearly coincides with the principal component of the second EOF mode already depicted in Figure 2. However, the freshwater event in 1999 which is consistently reproduced by the NAOSIM and the regional Kara Sea Model (see Figure 11) is the highest anomaly observed during the period 1950–2002. Although this single event can not be seen as an indication for a trend, it is of great importance whether those anomalies could occur more frequently or intensely in future. Further investigations should have a focus on these topics in order to assess possible changes on the Arctic Shelves.

[45] The effect of the discussed SLP anomaly on the local ice drift is similar to the effect on the freshwater dispersion. Owing to dominating easterly winds in winter 1998/1999, the export of sea ice to the north and east is significantly reduced. As a result, the duration of the ice period is prolonged and the ice volume increased, which is mainly owing to a more compact ice cover and less frequent open water (polynyas). This result is in remarkably good agreement with satellite observations. A more detailed investigation of this will follow.

[46] It is evident that our findings are in particular important for the local and regional scale. On the other hand, the delayed freshwater export from the Kara Sea in winter 1998/1999 highlights the potential of the Arctic Shelf areas to buffer the river discharge and modify the freshwater signal that enters the Arctic Ocean. The buffer capacity of Arctic Shelf Seas might be underestimated in global scale models owing to insufficient time and space resolution. The influence of shelf sea processes on large-scale distribution

of sea ice and freshwater in the Arctic Ocean awaits further investigation.

References

Backhaus, J. O. (1985), A three-dimensional model for the simulation of shelf sea dynamics, *Dtsch. Hydrogr. Z.*, *38*(H4), 165–187.

Gerdes, R., C. Köberle, and J. Willebrand (1991), The influence of numerical advection schemes on the results of ocean general circulation models, *Clim. Dyn.*, *5*, 211–226.

Gerdes, R., J. Hurka, M. Karcher, F. Kauker, and C. Koeberle (2005), Simulated history of convection in the Greenland and Labrador seas 1948–2001, in *Climate Variability of the Nordic Seas*, *Geophys. Monogr. Ser.*, vol. 158, edited by H. Drange et al., AGU, Washington, D. C., in press.

Gjevik, B., and T. Straume (1989), Model simulations of the M2 and the K1 tides in the Nordic Seas and the Arctic Ocean, *Tellus, Ser. A*, *41*, 73.

Haak, H., J. Jungclaus, U. Mikolajewicz, and M. Latif (2003), Formation and propagation of great salinity anomalies, *Geophys. Res. Lett.*, *30*(9), 1473, doi:10.1029/2003GL017065.

Häkkinen, S. (1999), A simulation of thermohaline effects of a great salinity anomaly, *J. Clim.*, *12*, 1781–1795.

Harms, I. H., and M. J. Karcher (1999), Modeling the seasonal variability of circulation and hydrography in the Kara Sea, *J. Geophys. Res.*, *104*(C6), 13,431–13,448.

Harms, I. H., M. J. Karcher, and D. Dethleff (2000), Modelling Siberian river runoff—Implications for contaminant transport in the Arctic Ocean, *J. Mar. Syst.*, *27*, 95–115.

Harms, I. H., U. Hübner, J. O. Backhaus, M. Kulakov, V. Stanovoy, O. Stepanets, L. Kodina, and R. Schlitzer (2003), Salt intrusions in Siberian river estuaries: Observations and model experiments in Ob and Yensiei, in *Siberian River Runoff in the Kara Sea: Characterisation, Quantification, Variability and Environmental Significance*, *Proc. Mar. Sci.*, vol. 6, edited by R. Stein et al., pp. 27–46, Elsevier, New York.

Harms, I. H., C. Schrum, and K. Hatten (2005), Numerical sensitivity studies on the variability of climate relevant processes in the Barents Sea, *J. Geophys. Res.*, *110*, C06002, doi:10.1029/2004JC002559.

Hibler, W. D., III (1979), A dynamic thermodynamic sea ice model, *J. Phys. Oceanogr.*, *9*, 815–846.

Kalnay, E., et al. (1996), The NCEP/NCAR 40-Year Reanalysis Project, *Bull. Am. Meteorol. Soc.*, *77*, 437–495.

Karcher, M., R. Gerdes, F. Kauker, and C. Köberle (2003a), Arctic warming: Evolution and spreading of the 1990s warm event in the Nordic Seas and the Arctic Ocean, *J. Geophys. Res.*, *108*(C2), 3034, doi:10.1029/2001JC001265.

Karcher, M. J., M. Kulakov, S. Pivovarov, U. Schauer, F. Kauker, and R. Schlitzer (2003b), Flow of Atlantic Water to the Kara Sea—Comparing model results with observations, in *Siberian River Runoff in the Kara Sea: Characterisation, Quantification, Variability and Environmental Significance*, *Proc. Mar. Sci.*, vol. 6, edited by R. Stein et al., pp. 47–69, Elsevier, New York.

Kauker, F., R. Gerdes, M. J. Karcher, C. Koeberle, and J. Lieser (2003), Variability of Northern Hemisphere sea ice: A combined analysis of model results and observations for the period 1978–2001, *J. Geophys. Res.*, *108*(C6), 3182, doi:10.1029/2002JC001573.

Kern, S., and I. H. Harms (2004), Polynya variability in Arctic Shelf areas as inferred from passive microwave imagery and numerical modeling, paper presented at International Symposium on Climate Change in the Arctic, Arctic Clim. Impact Assess., Reykjavik.

Kowalik, Z., and A. Y. Proshutinsky (1993), Diurnal tides in the Arctic Ocean, *J. Geophys. Res.*, *98*(C9), 16,449–16,468.

Kowalik, Z., and A. Y. Proshutinsky (1994), The Arctic Ocean Tides, in *The Polar Oceans and Their Role in Shaping the Global Environment*, *Geophys. Monogr. Ser.*, vol. 85, edited by O. M. Johannessen, R. D. Muench, and J. E. Overland, pp. 137–158, AGU, Washington, D. C.

Lemke, P., W. B. Owens, and W. D. Hibler (1990), A coupled sea ice mixed layer pycnocline model for the Wedell Sea, *J. Geophys. Res.*, *95*(C6), 9513–9525.

Levitus, S., and T. Boyer (1994), *World Ocean Atlas 1994*, vol. 4, *Temperature*, *NOAA Atlas NESDIS 4*, Natl. Oceanic and Atmos. Admin., Silver Spring, Md.

Levitus, S., R. Burgett, and T. Boyer (1994), *World Ocean Atlas 1994*, vol. 3, *Salinity*, *NOAA Atlas NESDIS 3*, Natl. Oceanic and Atmos. Admin., Silver Spring, Md.

Maykut, G. A. (1986), The surface heat and mass balance, in *Geophysics of Sea Ice*, *NATO ASI Ser. B: Phys.*, vol. 146, edited by N. Untersteiner, pp. 395–463, Plenum Press, New York.

NSIDA Environmental Working Group (1997), *Joint U. S. Russian Atlas of the Arctic Ocean: Oceanography Atlas for the Winter Period* [CD-ROM], Natl. Snow and Ice Data Cent., Univ. of Colo., Boulder.

Pacanowski, R. C. (1995), MOM 2 documentation, user's guide and reference manual, *GFDL Ocean Group Tech. Rep. 3*, Geophys. Fluid Dyn. Lab., Princeton Univ., Princeton, N. J.

Parkinson, C. L., and W. M. Washington (1979), A large-scale numerical model of sea ice, *J. Geophys. Res.*, *84*(C1), 311–337.

Pavlov, V. K., and S. L. Pfirman (1995), Hydrographic structure and variability of the Kara Sea: Implications for pollutant distribution, *Deep Sea Res., Part II*, *42*(6), 1369–1390.

Pavlov, V. K., M. Y. Kulakov, and V. Stanovoy (1993), Oceanographical description of the Kara and Barents sea, report to the IASAP, Int. Atomic Energy Agency, Vienna.

Peterson, B. J., R. M. Holmes, J. W. McClelland, C. J. Vörösmarty, R. B. Lammers, A. I. Shiklomanov, I. A. Shiklomanov, and S. Rahmstorf (2002), Increasing river discharge to the Arctic Ocean, *Science*, *298*, 2171–2173.

Schauer, U., H. Loeng, B. Rudels, V. K. Ozhigin, and W. Dieck (2002), Atlantic water flow through the Barents and Kara Seas, *Deep Sea Res., Part I*, *49*(12), 2281–2298.

Simstich, J., I. H. Harms, M. J. Karcher, H. Erlenkeuser, V. Stanovoy, L. Kodina, D. Bauch, and R. Spielhagen (2005), Recent freshening in the Kara Sea (Siberia) recorded by stable isotopes in Arctic bivalve shells, *J. Geophys. Res.*, *110*, C08006, doi:10.1029/2004JC002722.

Stronach, J. A., J. O. Backhaus, and T. S. Murty (1993), An update on the numerical simulation of oceanographic processes in the waters between Vancouver Island and the mainland: The GF8 model, Oceanogr. *Mar. Biol. Ann. Rev.*, *31*, 86 pp.

————————————

I. H. Harms, Zentrum für Meeres- und Klimaforschung, Institut für Meereskunde, Universität Hamburg, D-20146 Hamburg, Germany. (harms@ifm.uni-hamburg.de)

M. J. Karcher, Alfred-Wegener-Institut für Polar und Meeresforschung, Columbusstrasse, D-27515 Bremerhaven, Germany.